Vinylogous Tetrathiafulvalene (TTF) π-Electron Donors and Derived Radical Cations: ESR Spectroscopic, Magnetic, and X-ray Structural Studies

Martin R. Bryce* and Adrian J. Moore

Department of Chemistry, University of Durham, Durham, DH1 3LE, UK

Brian K. Tanner and Roger Whitehead

Department of Physics, University of Durham, Durham, DH1 3LE, UK

William Clegg

Department of Chemistry, University of Newcastle, Newcastle upon Tyne, NE1 7RU, UK

Fabian Gerson, Axel Lamprecht, and Susanne Pfenninger

Institut für Physikalische Chemie, Universität Basel, Klingelbergstrasse 80, CH-4056 Basel, Switzerland

Received August 9, 1994. Revised Manuscript Received March 11, 1996[⊗]

The properties of new 2,2′-ethanediylidene(1,3-dithiole) derivatives **5**, **6**, and **8**−**11** are reported. Cyclic voltammetric studies establish that they are efficient donor molecules, with the extended conjugation resulting in stabilization of dications, relative to tetrathiafulvalene TTF (**1**). Radical cations are generated by oxidation of the neutral compounds with trifluoroacetic acid or anhydrous silver perchlorate in dichloromethane, and their ESR and proton ENDOR spectra are reported. The bulk of the spin population resides in the central $S_2C{=}C{-}C{=}CS_2$ part of the π-system. The X-ray crystal structure of donor **6** reveals that the 2,2′-ethanediylidene(1,3-dithiole) framework is planar. Donor **6** forms a crystalline 1:1 charge-transfer complex with TCNQ, the X-ray crystal structure of which shows a mixed stack structure. A solution of this complex in acetonitrile exhibits ESR spectra of both radical ions, $\mathbf{6}^{\bullet+}$ and $TCNQ^{\bullet-}$. Static susceptibility data are reported for TCNQ complexes of some of these donors.

Introduction

The study of quasi-one-dimensional organic metals has progressed rapidly since the discovery[1] of the charge-transfer complex of tetrathiafulvalene (TTF, **1**, Chart 1) and tetracyano-*p*-quinodimethane (TCNQ, **2**).[2] The synthesis of new organochalcogen donors has remained at the forefront of research, with a few systems, notably bis(ethylenedithio)tetrathiafulvalene (BEDT−TTF, **3**), providing radical cation salts which are organic superconductors with T_c values as high as ca. 12 K.[3]

The incorporation of conjugated linking groups between the two 1,3-dithiole rings of TTF has been widely explored as a structural modification to the π-donor unit.[4] The rationale behind the design of TTF deriva-

Chart 1

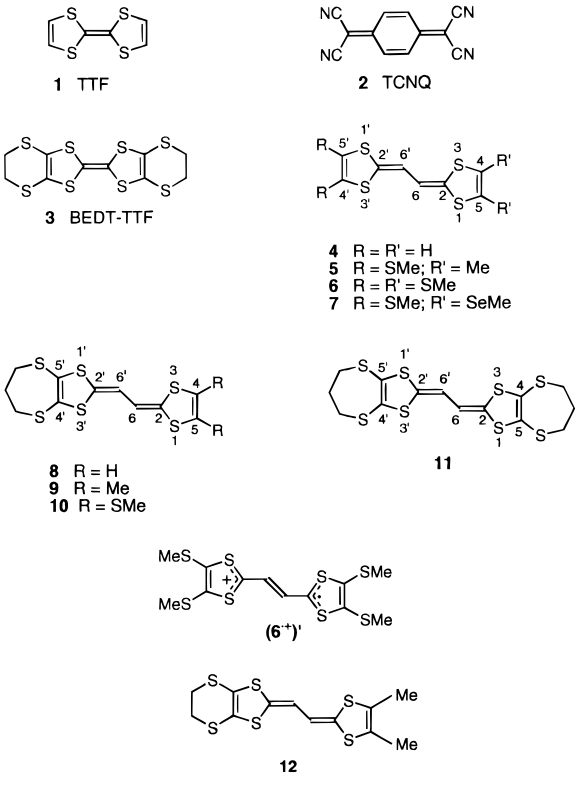

[⊗] Abstract published in *Advance ACS Abstracts,* May 1, 1996.

(1) (a) Ferraris, J. P.; Cowan, D. O.; Walatka, V.; Perlstein, J. H. *J. Am. Chem. Soc.* **1973,** *95,* 948. (b) Coleman, L. B.; Cohen, M. J.; Sandman, D. J.; Yamagishi, F. G.; Garito, A.F.; Heeger, A. J. *Solid State Commun.* **1973,** *12,* 1125.

(2) Recent reviews: (a) Ferraro, J. R.; Williams, J. M. *Introduction to Synthetic Electrical Conductors*; Academic Press: London, 1987. (b) Bryce, M. R. *Chem. Soc. Rev.* **1991**, *20,* 355. (c) Underhill, A. E. *J. Mater. Chem.* **1992,** *2,* 1.

(3) (a) Kini, A. M.; Geiser, U.; Wang, H. H.; Carlson, K. D.; Williams, J. M.; Kwok, W. K.; Vandervoot, K. G.; Thompson, J. E.; Stupka, D. L.; Jung, D.; Whangbo, M.-H. *Inorg. Chem.* **1990**, *29,* 2555. (b) Williams, J. M.; Ferraro, J. R.; Thorn, R. J.; Carlson, K. D.; Geiser, U.; Wang, H. H.; Kini, A. M.; Whangbo, M.-H. *Organic Superconductors (Including Fullerenes)*; Prentice Hall: Englewood Cliffs, NJ, 1992.

S0897-4756(94)00376-5 CCC: $12.00 Published 1996 by the American Chemical Society

tives with extended conjugation is that the oxidized states responsible for conduction in charge-transfer complexes and radical cation salts should be stabilized by decreased intramolecular Coulombic repulsion. There is now clear evidence from detailed solution electrochemical studies on several 2,2′-ethanediylidene(1,3-dithiole) derivatives, *e.g.*, the parent system **4**,[4b] that mainly the second oxidation potential is significantly lower than that of TTF **1**. One superconducting salt of a donor containing a vinylogous TTF framework has recently been reported,[4j] adding a new impetus to studies on these systems. In this paper we report new solution- and solid-state studies of radical cations of substituted 2,2′-ethanediylidene(1,3-dithiole) derivatives.

Experimental Section

The synthesis of compounds **5**, **6**, and **8**−**11** has been reported previously.[4f] Complexes of these donors with TCNQ **2** of 1:1 stoichiometry were obtained as detailed below.

General Procedure for Preparation of TCNQ Salts of the New Donors. The donor and TCNQ in equimolar amounts were dissolved separately in the minimum amount of hot dry solvent under nitrogen (dichloromethane was employed for **5** and **6**, and 1,1,2-trichloroethane for **8**−**11**). The two hot solutions were mixed and then allowed to cool to 20 °C to precipitate the charge-transfer complex, which was removed by filtration, washed with the solvent used and dried in vacuo. The 1:1 stoichiometry was determined by elemental analysis.

5−TCNQ. Obtained: C, 52.04; H, 3.21; N, 10.02%. Calculated for $C_{24}H_{18}N_4S_6$: C, 51.96; H, 3.27; N, 10.10%.

6−TCNQ. Obtained: C, 46.69; H, 2.83; N, 8.99%. Calculated for $C_{24}H_{18}N_4S_8$: C, 46.57; H, 2.93; N, 9.05%.

8−TCNQ. Obtained: C, 51.20; H, 2.78; N, 10.50%. Calculated for $C_{23}H_{14}N_4S_6$: C, 51.27; H, 2.62; N, 10.40%.

9−TCNQ. Obtained: C, 53.01; H, 3.32; N, 9.96%. Calculated for $C_{25}H_{18}N_4S_6$: C, 52.97; H, 3.20; N, 9.88%.

10−TCNQ. Obtained: C, 47.50; H, 2.96; N, 8.94%. Calculated for $C_{25}H_{18}N_4S_8$: C, 47.50; H, 2.88; N, 8.88%.

11−TCNQ. Obtained: C, 48.63; H, 2.75; N, 8.84%. Calculated for $C_{26}H_{18}N_4S_8$: C, 48.57; H, 2.82; N, 8.71%.

Conductivity measurements were obtained on compressed pellets using standard two-probe techniques and apparatus described previously.[5] Cyclic voltammograms were registered on a Metrohm Polarecord E 506 instrument with a VA-Scanner E 612/VA Stand 663. ESR spectra were taken on a Varian E-9 instrument, while a Bruker ESP 300 system served for the ENDOR and TRIPLE resonance studies. Magnetic susceptibility data were obtained using an Oxford Instruments 5 T Faraday balance.

X-ray crystallographic measurements on compound **6** and complex **6**−TCNQ were made at 240 K on a Stoe-Siemens diffractometer fitted with a Cryostream cooler,[6] using graphite-monochromated Cu Kα radiation (λ = 1.541 84 Å). Crystallographic data are given in Table 1, and atomic coordinates are given in Tables 2 and 3. Cell parameters were refined from the 2θ values of 30−32 reflections in the range 40−45°, measured at ±ω to minimize systematic errors. Intensities were measured with ω/θ scans and an on-line profile-fitting procedure,[7] to a maximum 2θ of 130°. No significant intensity variation was observed for three standard reflections measured at regular intervals. Each data set consists of a complete unique set of reflections, together with some symmetry-equivalent reflections; for the noncentrosymmetric *C*2 structure of the TCNQ complex, a complete set of Friedel opposites was collected. Semiempirical absorption corrections were applied, based on sets of equivalent reflections measured at a range of azimuthal angles.[8] The apparent pseudohexagonal nature of the unit cell for **6**−TCNQ, indicated by the cell parameters, is illusory, because of the lattice C centering, which renders the *a* and *c* axes completely inequivalent even in purely geometric terms.

Table 1. Crystallographic Data

compound	**6**	**6**−TCNQ
formula	$C_{12}H_{14}S_8$	$C_{28}H_{18}N_4S_8$
M	414.71	666.94
crystal system	triclinic	monoclinic
space group	$P\bar{1}$	*C*2
a (Å)	5.1116(8)	15.552(2)
b (Å)	7.9995(14)	6.7345(10)
c (Å)	11.277(2)	15.620(2)
α (deg)	92.378(11)	90
β (deg)	94.110(14)	120.078(7)
γ (deg)	107.076(11)	90
V (Å^3)	438.73(13)	1415.7(3)
Z	1	2
D_c (g cm^{-3})	1.570	1.565
μ (mm^{-1})	9.311	6.072
F(000)	214	684
crystal size (mm)	0.80 × 0.32 × 0.05	0.48 × 0.40 × 0.40
crystal color	yellow	black
maximum *hkl* indexes	6, 9, 13	18, 7, 18
transmission	0.125−0.820	0.197−0.393
reflections measured	1584	2836
unique reflections	1257	2333
R_{int}	0.094	0.077
weighting parameters *a*, *b*	0.0828, 0.1872	0.1637, 1.6860
extinction coefficient *x*	0.047(4)	0.030(2)
no. of refined parameters	94	166
*wR*2 (all data)	0.119	0.187
*R*1 (observed data)	0.044 (1219)	0.069 (2321)
goodness of fit	1.08	1.06
Max, min electron density (eÅ^{-3})	0.40, −0.47	0.59, −0.72

Table 2. Atomic Coordinates (×10^4) for Compound 6 (For the Numbering of Atoms, See Figure 6a)

	x	*y*	*z*
S(1)	914(2)	10398.0(9)	7091.3(7)
S(2)	−2342(2)	6859.5(11)	8590.1(7)
S(3)	3249.2(14)	7914.1(9)	5782.9(6)
S(4)	371.8(13)	4873.9(8)	7047.6(5)
C(1)	4281(7)	11463(4)	7791(4)
C(2)	216(9)	7415(6)	9857(3)
C(3)	1136(5)	8269(3)	6866(2)
C(4)	−173(5)	6873(4)	7448(2)
C(5)	2756(5)	5688(3)	6017(2)
C(6)	4029(5)	4684(3)	5428(2)

(4) (a) Yoshida, Z.; Kawase, T.; Awaji, H.; Sugimoto, I.; Sugimoto, T.; Yoneda, S. *Tetrahedron Lett.* **1983,** *24*, 3469. (b) Sugimoto, T.; Awaji, H.; Sugimoto, I.; Misaki, Y.; Kawase, T.; Yoneda, S.; Yoshida, Z. *Chem. Mater.* **1989,** *1*, 535. (c) Moore, A. J.; Bryce, M. R.; Ando, D. J.; Hursthouse, M. B. *J. Chem. Soc., Chem. Commun.* **1991**, 320. (d) Hansen, T. K.; Lakshimikantham, M. V.; Cava, M. P.; Metzger, R. M.; Becher, J. *J. Org. Chem.* **1991**, *56*, 2720. (e) Khanous, A.; Gorgues, A.; Texier, F. *Tetrahedron Lett.* **1990,** *31*, 7307. (f) Moore, A. J.; Bryce, M. R. *Tetrahedron Lett.* **1992,** *33*, 1373. (g) Bryce, M. R.; Coffin, M. A.; Clegg, W. *J. Org. Chem.* **1992,** *57*, 1696. (h) Sallé, M.; Jubault, M.; Gorgues, A.; Boubekeur, K.; Fourmigué, M.; Batail, P.; Canadell, E. *Chem. Mater.* **1993**, *5*, 1196. (i) Terahara, A.; Ohya-Nishiguchi, H.; Hirota, N.; Awaji, H.; Kawase, T.; Yoneda, S.; Sugimoto, T.; Yoshida, Z. *Bull. Chem. Soc. Jpn.* **1984**, *57*, 1760. (j) Misaki, Y.; Higuchi, N.; Fujiwara, H.; Yamabe, T.; Mori, T.; Mori, H.; Tanaka, S. *Angew. Chem., Int. Ed. Engl.* **1995**, *34*, 1222. (k) Misaki, Y.; Ohta, T.; Higuchi, N.; Fujiwara, H.; Yamabe, T.; Mori, T.; Mori, H.; Tanaka, S. *J. Mater. Chem.* **1995**, *5*, 1571. (l) For a review see: Bryce, M. R. *J. Mater. Chem.* **1995**, *5*, 1481.

(5) Wudl, F.; Bryce, M. R. *J. Chem. Educ.* **1990,** *67*, 717.

(6) Cosier, J.; Glazer, A. M. *J. Appl. Crystallogr.* **1986**, *19*, 105.

(7) Clegg, W. *Acta Crystallogr.* **1981**, *A37*, 22.

(8) Sheldrick, G. M. *SHELXTL/PC Manual*; Siemens Analytical X-Ray Instruments Inc., Madison, WI, 1990.

Table 3. Atomic Coordinates ($\times 10^4$) for the Complex 6−TCNQ (For the Numbering of Atoms, See Figure 7a)

	x	*y*	*z*
S(1)	2991.6(11)	2508(2)	693.1(8)
S(2)	5312.2(10)	3334(2)	1246.6(9)
S(3)	3772.8(8)	2614(2)	2889.7(7)
S(4)	5802.9(8)	3309(2)	3366.5(7)
C(1)	2053(4)	1371(10)	869(4)
C(2)	5985(7)	1095(12)	1369(6)
C(3)	3984(4)	2673(8)	1892(3)
C(4)	4935(4)	2970(7)	2120(3)
C(5)	5003(3)	2966(6)	3807(3)
C(6)	5320(3)	3002(7)	4806(3)
C(7)	5227(3)	7765(8)	4228(3)
C(8)	5990(3)	7747(8)	5244(3)
C(9)	4229(3)	7721(8)	4019(3)
C(10)	5461(4)	7849(7)	3465(3)
C(11)	6452(4)	8137(9)	3671(4)
C(12)	4715(4)	7744(8)	2453(4)
N(1)	7245(4)	8422(12)	3849(4)
N(2)	4114(4)	7630(9)	1634(3)

Both structures were determined by automatic direct methods[8] and refined[9] by least-squares on F^2, with a weighting scheme $w^{-1} = \sigma^2(F_o^2) + (aP)^2 + bP$, where $P = (F_o^2 + 2F_c^2)/3$. The extinction correction multiplies F by $(1 + 0.001xF_c^2\lambda^3/\sin 2\theta)^{1/4}$, where x is a refined isotropic extinction coefficient. The absolute structure for the TCNQ complex was established by refinement of the enantiopole parameter[10] to a value of 0.08(4), insignificantly different from its ideal value of zero. All shift/esd values in the final cycles of refinement were <0.001. All non-hydrogen atoms were refined anisotropically, and hydrogen atoms were constrained in both geometry and isotropic displacement.

The residual $wR2 = [\sum w(F_o^2 - F_c^2)^2/\sum w(F_o^2)^2]^{1/2}$ for all data; for comparison with conventional refinements on F, $R1 = \sum||F_o| - |F_c||/\sum|F_o|$ for reflections having $F_o^2 > 2\sigma(F_o^2)$. The goodness of fit is calculated on F^2 values.

Anisotropic displacement parameters and hydrogen atom coordinates are available as supporting information.

Results and Discussion

Electrochemical Properties. The solution redox properties of donors **5**, **6**, and **8**−**11** have been studied by cyclic voltammetry in dichloromethane solution, and the results are collated in Table 4, along with selected model compounds for comparison. All the new compounds undergo two, separate, one-electron oxidations (i.e., sequential formation of the radical cation and the dication species) in the range 0.3−1.0 V vs Ag/AgCl. Both waves are reversible, the difference between anodic and cathodic peaks being 60 ± 5 mV.[11] These data are entirely consistent with previous work vinylogous on TTF systems which has established that "stretching" the TTF molecule by insertion of a vinyl group, viz. molecule **4**,[4a,b] lowers significantly the potential of the second redox wave and reduces the difference between the values of $E_1^{1/2}$ and $E_2^{1/2}$. Similar behavior is observed for the new systems described herein. The increased stabilization of the dication state is understood in terms of increased separation of the two positive charges, relative to the TTF dication, as discussed previously.[4b,c] Compounds **5** and **9** are, predictably, the best donors in the series due to the presence of electron-releasing methyl substituents on the 1,3-dithiole ring.

(9) Sheldrick, G. M. *SHELXL-93*, program for crystal structure refinement, University of Göttingen, 1993.
(10) Flack, H. D. *Acta Crystallogr.* **1983**, *A39*, 876.
(11) Bard, A. J.; and Faulkner, L. R. *Electrochemical Methods: Fundamentals and Applications*; Wiley, New York, 1980; Chapter 6.

Table 4. Half-Wave Oxidation Potentials Determined by Cyclic Voltammetry for New Vinylogous Donors and Model Compounds[a] and Conductivity Data[b] and IR (C≡N) Stretching Frequencies for TCNQ Complexes[c]

donor	$E_1^{1/2}$, V	$E_2^{1/2}$, V	ΔE, V	conductivity σ_{rt}, S cm^{-1}	ν_{max}(C≡N), cm^{-1}
1	0.395	0.790	0.395		
3	0.599	0.922	0.323		
5	0.407	0.591	0.184	5×10^{-4}	2197
6	0.508	0.631	0.123	1×10^{-9}	2148, 2175, 2195
8	0.462	0.668	0.206	4×10^{-5}	2196
9	0.408	0.624	0.216	4×10^{-5}	2197
10	0.513	0.660	0.147	7×10^{-7}	2180, 2200
11	0.519	0.697	0.178	6×10^{-8}	2177, 2199

[a] Experimental conditions: donor (ca. 1×10^{-5} mol dm^{-3}) electrolyte $Bu_4N^+ClO_4^-$ (*ca.* 1×10^{-1} mol dm^{-3}) in dichloromethane, 25 °C, vs Ag/AgCl (3 M KCl), working electrode Pt disk, counter electrode Pt wire, experimental error ±0.005 V. The values given here are mostly shifted to more positive potentials relative to those reported previously,[4f] this shift being presumably due to the slightly higher water content of the solvent. [b] Two-probe compressed pellet measurement. [c] KBr disk. Sharp peaks were observed for TCNQ complexes of donors **6**, **10**, and **11**, whereas the complexes of donors **5**, **8**, and **9** displayed broad peaks, typical of an organic semiconductor.

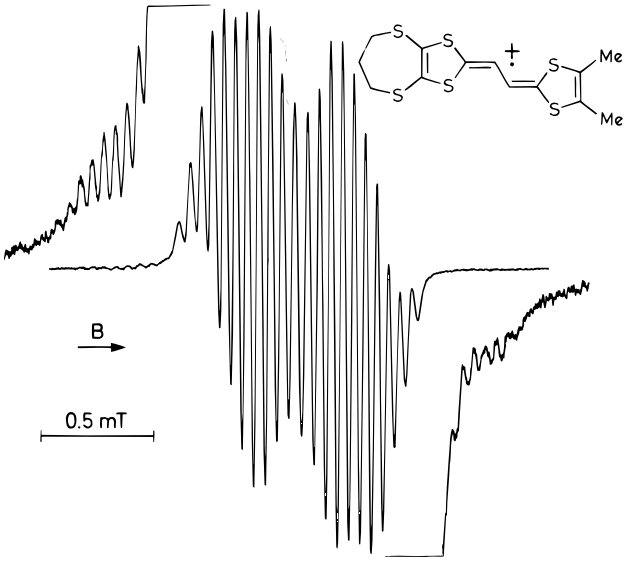

Figure 1. ESR spectrum of $\mathbf{9}^{\cdot+}$. Solvent, CH_2Cl_2; counterion ClO_4^-; temperature 233 K. The signals at the peripheries of the spectrum have been amplified to make the ^{33}S satellites more evident.

ESR/ENDOR Studies. For spectroscopic studies, the radical cations derived from **5**, **6**, and **8**−**11** were generated by oxidation of the corresponding neutral compounds with trifluoroacetic acid or anhydrous silver perchlorate in dichloromethane. At 195 K, their concentration did not significantly diminish for several days. The ESR and proton ENDOR spectra were taken in the range 203−298 K. They are exemplified in Figures 1−3 by those of $\mathbf{9}^{\cdot+}$ (ESR), $\mathbf{11}^{\cdot+}$ (ESR), and $\mathbf{8}^{\cdot+}$ (ENDOR). With the exception of $\mathbf{5}^{\cdot+}$, the ESR spectra of all radical cations displayed satellites due to ^{33}S nuclei in natural abundance. The proton and ^{33}S coupling constants, a_H and a_S in millitesla, and g factors of $\mathbf{4}^{\cdot+}$− $\mathbf{6}^{\cdot+}$, and $\mathbf{8}^{\cdot+}$−$\mathbf{11}^{\cdot+}$ are listed in Table 5. The $|a_H|$ values were derived from the frequencies of ENDOR signals and verified by simulations of the ESR spectra. The larger of them ($|a_H| > 0.1$ mT) decreased slightly on raising the temperature.

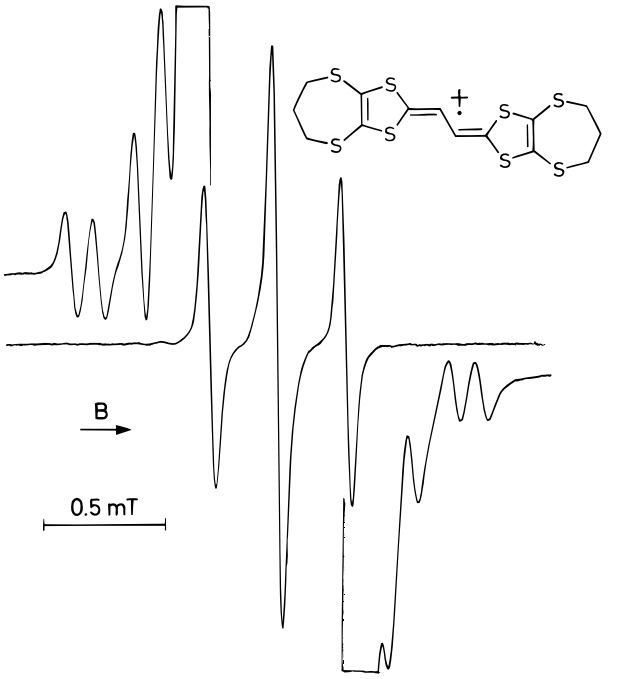

Figure 2. ESR spectrum of $\mathbf{11}^{\cdot+}$. Solvent, CH_2Cl_2; counterion $CF_3CO_2^-$; temperature 273 K. The signals at the peripheries of the spectrum have been amplified to make the ^{33}S satellites more evident.

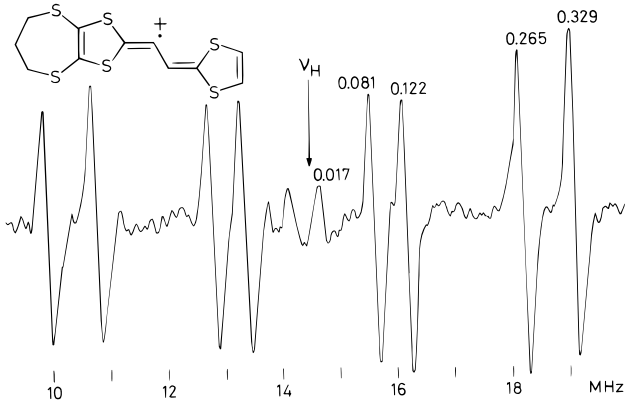

Figure 3. Proton ENDOR spectrum of $\mathbf{8}^{\cdot+}$. Solvent, CH_2Cl_2; counterion ClO_4^-; temperature, 203 K. The numbers above the signals are the absolute values of the proton coupling constants in millitesla.

Assignments of the coupling constants to protons and ^{33}S nuclei in the individual positions of $\mathbf{5}^{\cdot+}$, $\mathbf{6}^{\cdot+}$, and $\mathbf{8}^{\cdot+}$–$\mathbf{11}^{\cdot+}$ are based on spin populations calculated by the McLachlan procedure[12] (with the use of conventional Hückel heteroatom parameters[13]) and on the AM1 method[14] starting from the MMX-specified geometry.[15] They also comply with the assignments made for corresponding values of $\mathbf{4}^{\cdot+}$ and some of its derivatives by other authors.[4i] The signs, as indicated by theory, are in agreement with those derived from general-TRIPLE resonance experiments performed on the ENDOR signals.[16]

The spin distribution in the π-system of $\mathbf{4}^{\cdot+}$ is similar to that in the TTF radical cation[13] (Figure 4). The bulk of the spin population in $\mathbf{4}^{\cdot+}$ and its derivatives $\mathbf{5}^{\cdot+}$, $\mathbf{6}^{\cdot+}$, and $\mathbf{8}^{\cdot+}$–$\mathbf{11}^{\cdot+}$ resides in the central $S_2C{=}C{-}C{=}CS_2$ part of the π-system with only slight delocalization on the substituent groups. Consequently, the observed substantial coupling constants a_S arise from the four ^{33}S nuclei in the "inner" thiafulvene moieties, whereas such isotopes in the SMe substituents, or in the "outer" rings, have a_S values too small to give rise to observable satellites. This statement is analogous to that made for the ^{33}S coupling constants in the ESR spectra of the BEDT–TTF (**3**) radical cation.[13]

Solid-state ESR studies on the complex **6**–TCNQ gave a strong ESR signal of nearly 6 mT width at room temperature. The ESR spectrum of the complex obtained in anhydrous acetonitrile at room temperature, with exclusion of oxygen, clearly showed the contributions of both radical ions, $\mathbf{6}^{\cdot+}$ (this work) and $TCNQ^{\cdot-}$ [17] (Figure 5). Their relative concentrations are consistent with their formation from a 1:1 **6**–TCNQ complex.

X-ray Structural Studies. The molecular structure of donor **6** and its 1:1 complex with TCNQ have been determined by single-crystal X-ray analysis (Figures 6 and 7, respectively). Bond lengths and angles for donor **6** and the complex **6**–TCNQ are given in Tables 6 and 7, respectively. Compound **6** is isostructural with compound **7**[4g] in which two of the methylthio groups are replaced by methylseleno groups. The key feature of the structure of **6** is that the 2,2′-ethanediylidenebis-(1,3-dithiole) framework is planar. The molecule is in the *transoid* conformation, which was expected for steric reasons; this is consistent with the interpretation by Sugimoto et al. of spectroscopic data for the unsubstituted analogue **4**,[4b] and with the X-ray crystal structure of **12** which we have reported previously.[4c] Molecules of compound **6** stack in a uniform fashion along the *x* axis (Figure 6b).

The crystal structure of the charge-transfer complex **6**–TCNQ is shown in Figure 7. This is the first crystal structure of a charge-transfer complex of a donor possessing the 2,2′-ethanediylidenebis(1,3-dithiole) framework. The donor and acceptor units pack in an alternating mixed stack motif, which explains the low conductivity value of this material (Table 4). The donor–acceptor interplanar distances are alternately 3.228 and 3.497 Å. The mode of overlap can be seen in Figure 7c, which also shows that the adjacent stacks are well separated by their substituent groups. Both the donor and the acceptor species in the complex have an exact C_2 axis of symmetry. The oxidized donor molecule in the complex is not planar; the two 1,3-dithiole rings form a dihedral angle of 19°. Analysis of the bond lengths of donor moiety **6** provides evidence for the charge and spin populations affecting the central $S_2C{=}C{-}C{=}CS_2$ part of the π-system in the complex **6**–TCNQ, in agreement with the results of the solution ESR study discussed above. Notably, the C(5)–C(6) bond is lengthened, and the C(6)–C(6′) bond is shortened in the complex, compared with the neutral molecule **6** (Tables 6 and 7). The S(3)–C(5) and S(4)–C(5) bonds are also shortened in the complex. These

(12) McLachlan, A. D. *Mol. Phys.* **1960**, *3*, 233.
(13) Cavara, L.; Gerson, F.; Cowan, D. O.; Lerstrup, K. *Helv. Chim. Acta* **1986,** *69*, 141.
(14) Dewar, M. J. S.; Zoebisch, E. G.; Healy, E. F.; Stewart, J. J. P. *J. Am. Chem. Soc.* **1985,** *107*, 3902.
(15) Derived from MM2 (QCPE-395) force field with the π-VESCF routines taken from MMP1 (QCPE-318), both by N. L. Allinger.
(16) Kurreck, H.; Kirste, B.; Lubitz, W. *Electron Nuclear Double Resonance Spectroscopy of Radicals in Solution*; VCH Publishers: New York, 1988; Chapter 2.
(17) Gerson, F.; Heckendorn, R; Cowan, D. O.; Kini, A. M.; Maxfield, M. *J. Am. Chem. Soc.* **1983**, *105*, 7017.

Table 5. Proton and ^{33}S Coupling Constants, a_H and a_S (in millitesla), and g Factors for $4^{\cdot+}$–$6^{\cdot+}$ and $8^{\cdot+}$–$11^{\cdot+}$ [a] (For the Numbering of Atoms, See Formulas 4–6 and 8–11)[b]

radical cation	temp (K)	a_H	position	a_S	position	g
4$^{\cdot+}$[c]	193	−0.313 (2H)	6,6′-H	+0.398 (2S)	1,1′	2.0081
		−0.123 (2H)	4,4′-H	*d*		
		−0.082 (2H)	5,5′-H			
5$^{\cdot+}$	223	−0.351 (1H)	6′-H	*e*		2.0077
		−0.220 (1H)	6-H			
		+0.094 (3H)	4-Me			
		+0.050 (3H)	5-Me			
		+0.019 (3H)	S−Me			
		+0.013 (3H)	S−Me			
6$^{\cdot+}$	253	−0.272 (2H)	6,6′-H	+0.383 (2S)	1,1′	2.0079
		+0.024 (6H)	S−Me	+0.296 (2S)	3,3′	
		+0.015 (6H)	S−Me			
8$^{\cdot+}$	203	−0.329 (1H)	6′-H	+0.39 ± 0.02 (2S)	1,1′	2.0079
		−0.265 (1H)	6-H	*d*		
		−0.122 (1H)	4-H			
		−0.081 (1H)	5-H			
		+0.017 (2H)	S−CH_2			
		<0.010 (2H)	S−CH_2			
		<0.010 (2H)	S−CH_2−CH_2			
9$^{\cdot+}$	203	−0.378 (1H)	6′-H	+0.38 ± 0.02 (2S)	1,1′	2.0079
		−0.202 (1H)	6-H	*d*		
		+0.104 (3H)	4-Me			
		+0.053 (3H)	5-Me			
		+0.016 (2H)	S−CH_2			
		<0.010 (2H)	S−CH_2			
		<0.010 (2H)	S−CH_2−CH_2			
10$^{\cdot+}$	253	−0.307 (1H)	6′-H[f]	+0.384 (2S)	1,1′	2.0079
		−0.255 (1H)	6-H[f]	+0.338 (2S)	3,3′	
		+0.026 (3H)	S−Me			
		+0.017 (3H)	S−Me			
		+0.017 (2H)	S−CH_2			
		<0.010 (2H)	S−CH_2			
		<0.010 (2H)	S−CH_2−CH_2			
11$^{\cdot+}$	253	−0.288 (2H)	6,6′-H	+0.383 (2S)	1,1′	2.0078
		+0.017 (4H)	S−CH_2	+0.320 (2S)	3,3′	
		<0.010 (4H)	S−CH_2			
		<0.010 (4H)	S−CH_2−CH_2			

[a] Experimental error if not explicitly indicated: ±0.002 and ±0.001 in $|a_H|$ larger and smaller, respectively, than 0.1 mT, ±0.005 mT in a_S, and ±0.0001 in g. [b] This numbering accords to the IUPAC rules and differs from that used in the X-ray crystallographic structure analysis of **6** and **6**−TCNQ (Figures 6a and 7a). [c] Reference 4i. [d] Only the ^{33}S satellites with the larger a_S value detected. [e] No ^{33}S satellites detected. [f] Assignment uncertain.

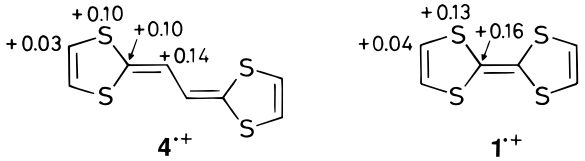

Figure 4. π-spin populations in **4**$^{\cdot+}$, as compared with those in the TTF radical cation **1**$^{\cdot+}$. These values have been derived by combining experimental findings with the results of calculations by the McLachlan procedure.[12]

data imply that canonical form (**6**$^{\cdot+}$)′ is an important contributor to the overall structure of the radical cation **6**$^{\cdot+}$.

Analysis of the bond lengths of the TCNQ moiety in TCNQ salts is frequently employed for determining the degree of charge transfer, as neutral TCNQ and anionic TCNQ have significantly different bond lengths.[18] The data for complex **6**−TCNQ (Table 7) are entirely consistent with the presence of the TCNQ radical anion. Notably, the bond lengths C(8)−C(9′) (1.355 Å), C(7)−C(8) (1.427 Å), and C(10)−C(11) (1.421 Å) are signatures of $TCNQ^{\cdot-}$ (1.362, 1.424, and 1.417 Å, respectively, in

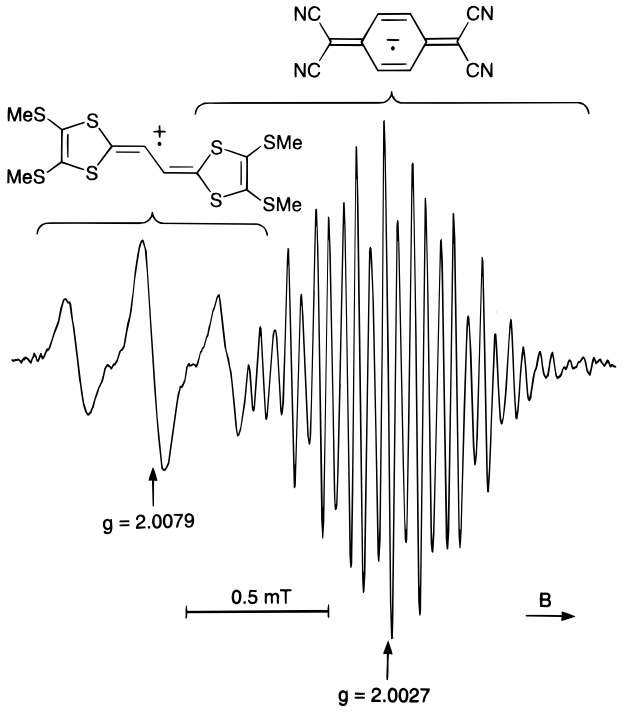

Figure 5. ESR spectrum of the complex **6**−TCNQ in acetonitrile solution at 295 K.

(18) (a) Ashwell, G. J.; Wallwork, S. C.; Baker, S. R.; Berthier, P. I. C. *Acta Crystallogr.* **1975**, *B31*, 1174. (b) Bryce, M. R.; Ahmad, M. M.; Friend, R. H.; Obertelli, D.; Fairhurst, S. A.; Winter, J. N. *J. Chem. Soc., Perkin Trans. 2* **1988,** 1151. (c) Umland, T. C.; Allie, S.; Kuhlmann, T.; Coppens, P. *J. Phys. Chem.* **1988,** *92*, 6456.

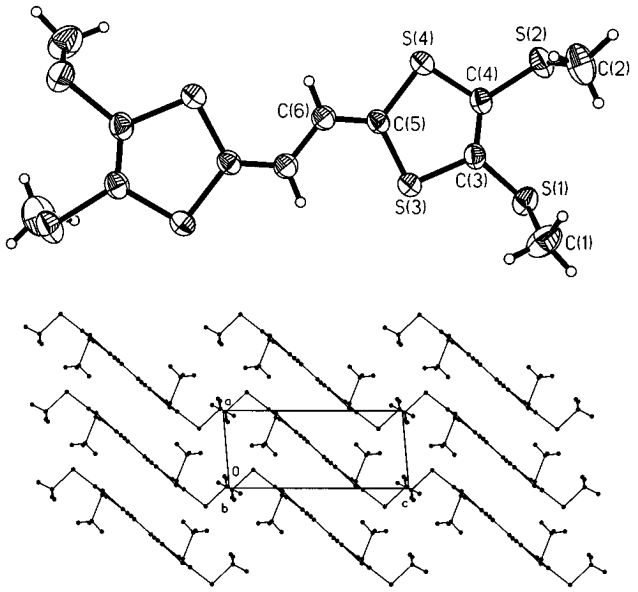

Figure 6. X-ray crystal structure of compound **6** (a, top) showing crystallographic atom numbering scheme (50% probability ellipsoids); (b, bottom) showing the packing of the molecules.

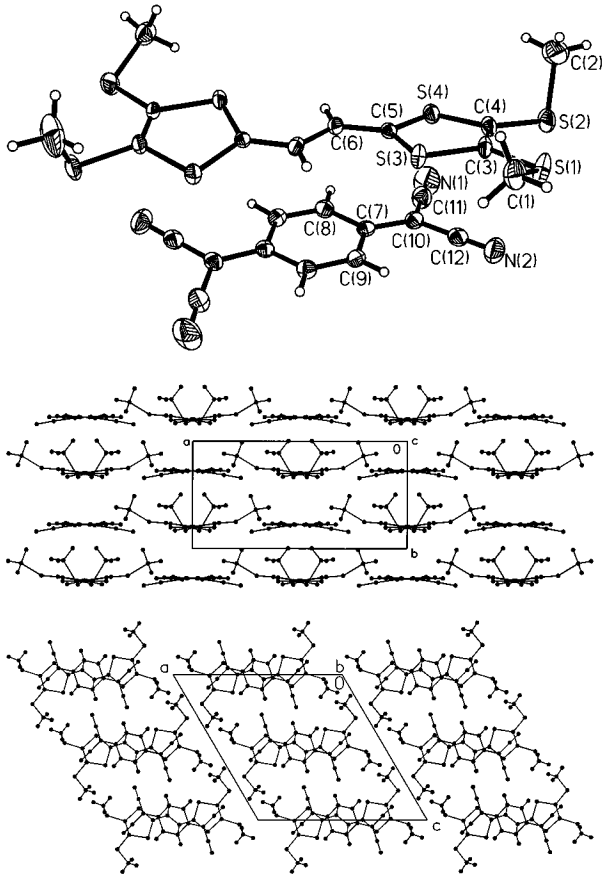

Figure 7. X-ray crystal structure of complex **6**−TCNQ (a, top) showing the crystallographic atom numbering scheme (50% probability ellipsoids); (b, middle) showing the packing as seen projected along the *c* axis; (c, bottom) projected along the *b* axis.

cation−$TCNQ^{\cdot-}$ salts of 1:1 stoichiometry), whereas the corresponding bond lengths in neutral TCNQ are 1.346, 1.448, and 1.440 Å, respectively. This conclusion is supported by the IR spectroscopic data for the TCNQ complexes (Table 4) for which the nitrile stretching

Table 6. Bond Lengths (Å) and Bond Angles (deg) for Compound 6 (For the Numbering of Atoms, See Figure 6a)[a]

S(1)−C(3)	1.749(3)	S(1)−C(1)	1.789(3)
S(2)−C(4)	1.757(3)	S(2)−C(2)	1.813(3)
S(3)−C(3)	1.755(3)	S(3)−C(5)	1.758(3)
S(4)−C(4)	1.749(3)	S(4)−C(5)	1.749(3)
C(3)−C(4)	1.346(4)	C(5)−C(6)	1.355(4)
C(6)−C(6′)	1.434(5)		
C(3)−S(1)−C(1)	99.83(14)	C(4)−S(2)−C(2)	99.1(2)
C(3)−S(3)−C(5)	96.04(13)	C(4)−S(4)−C(5)	96.37(12)
C(4)−C(3)−S(1)	125.9(2)	C(4)−C(3)−S(3)	116.9(2)
S(1)−C(3)−S(3)	117.3(2)	C(3)−C(4)−S(4)	117.0(2)
C(3)−C(4)−S(2)	126.5(2)	S(4)−C(4)−S(2)	116.5(2)
C(6)−C(5)−S(4)	123.2(2)	C(6)−C(5)−S(3)	123.3(2)
S(4)−C(5)−S(3)	113.50(14)	C(5)−C(6)−C(6′)	124.3(3)

[a] Symmetry transformation for primed atoms: $-x+1, -y+1, -z+1$.

Table 7. Bond lengths (Å) and Bond Angles (deg) for the Complex 6−TCNQ (For the Numbering of Atoms, See Figure 7a)[a]

S(1)−C(3)	1.733(4)	S(1)−C(1)	1.787(6)
S(2)−C(4)	1.752(4)	S(2)−C(2)	1.790(7)
S(3)−C(5)	1.739(4)	S(3)−C(3)	1.746(4)
S(4)−C(5)	1.713(4)	S(4)−C(4)	1.741(5)
C(3)−C(4)	1.351(7)	C(5)−C(6)	1.380(6)
C(6)−C(6′)	1.402(9)	C(7)−C(10)	1.413(6)
C(7)−C(9)	1.416(6)	C(7)−C(8)	1.427(6)
C(8)−C(9′)	1.355(6)	C(9)−C(8′)	1.355(6)
C(10)−C(12)	1.418(7)	C(10)−C(11)	1.421(7)
C(11)−N(1)	1.137(7)	C(12)−N(2)	1.148(7)
C(3)−S(1)−C(1)	102.4(2)	C(4)−S(2)−C(2)	101.8(3)
C(5)−S(3)−C(3)	96.4(2)	C(5)−S(4)−C(4)	96.9(2)
C(4)−C(3)−S(1)	123.9(3)	C(4)−C(3)−S(3)	116.0(3)
S(1)−C(3)−S(3)	119.9(3)	C(3)−C(4)−S(4)	116.6(3)
C(3)−C(4)−S(2)	124.4(4)	S(4)−C(4)−S(2)	118.5(3)
C(6)−C(5)−S(4)	122.1(3)	C(6)−C(5)−S(3)	123.8(3)
S(4)−C(5)−S(3)	114.1(2)	C(5)−C(6)−C(6′)	124.1(5)
C(10)−C(7)−C(9)	121.5(4)	C(10)−C(7)−C(8)	121.0(4)
C(9)−C(7)−C(8)	117.5(4)	C(9′)−C(8)−C(7)	121.4(4)
C(8′)−C(9)−C(7)	121.1(4)	C(7)−C(10)−C(12)	121.7(4)
C(7)−C(10)−C(11)	121.5(4)	C(12)−C(10)−C(11)	116.7(4)
N(1)−C(11)−C(10)	177.9(7)	N(2)−C(12)−C(10)	179.0(6)

[a] Symmetry transformation for primed atoms: $-x+1, y, -z+1$.

frequencies are all consistent with anionic TCNQ.[19]

Magnetic Susceptibility Studies on TCNQ Complexes. Measurements of the static magnetization of a number of TCNQ charge-transfer complexes have been made over the temperature range 4.2−300 K in fields of up to 5 T using a Faraday balance magnetometer. The complex which yielded crystals of sufficient size for crystal structure analysis, **6**−TCNQ, exhibited diamagnetic behavior across the entire temperature range. This result was reproduced on three different samples of the complex, prepared from two separate batches of donor **6**. This is explained by spin pairing of the radicals within the mixed donor−acceptor stacks, the measured value of the diamagnetic susceptibility being $\chi_{dia}^{exp} = -2.8\ (\pm 0.4) \times 10^{-4}$ emu mol^{-1} which agrees with that calculated from the Pascal constants of $\chi_{dia}^{calc} = -2.93 \times 10^{-4}$ emu mol^{-1}.

The complex **11**−TCNQ was also diamagnetic; the measured susceptibility $\chi_{dia}^{exp} = -2.3\ (\pm 0.6) \times 10^{-4}$ emu mol^{-1} was somewhat lower than the value of $\chi_{dia}^{calc} = -3.05 \times 10^{-4}$ emu mol^{-1} calculated from the Pascal constants.

(19) Chappel, J. S.; Bloch, A. N.; Bryden, W. A.; Maxfield, M.; Poehler, T. O.; Cowan, D. O. *J. Am. Chem. Soc.* **1981**, *103*, 2442.

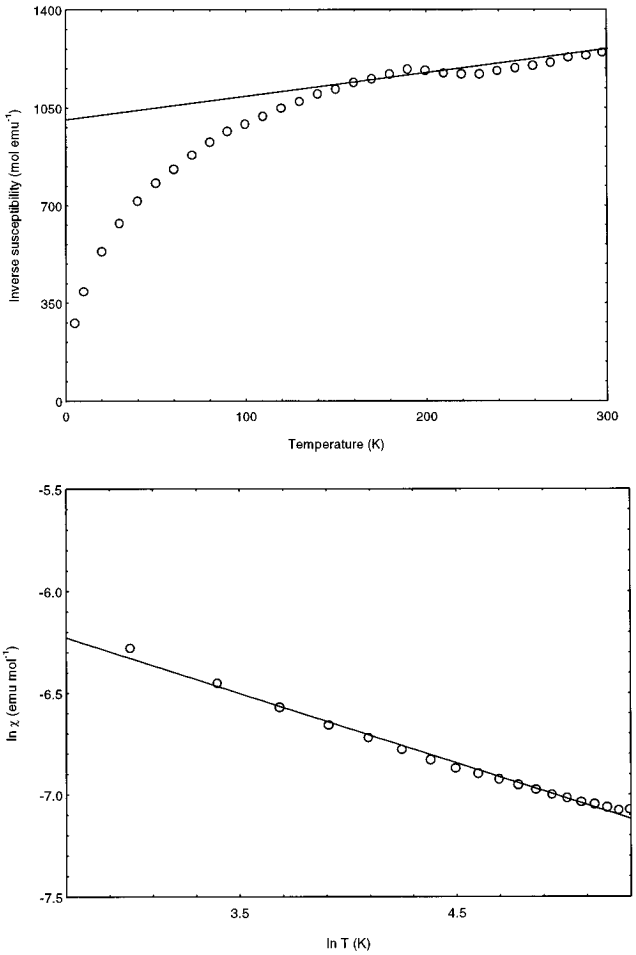

Figure 8. (a, top) Inverse susceptibility of **9**−TCNQ as a function of temperature (b, bottom) ln χ versus ln T plot for the same compound, showing power-law behavior $\chi = mT^{-a}$ where $\alpha = 0.34 \pm 0.01$ over the temperature range 15−200 K.

The complex **9**−TCNQ was found to be weakly paramagnetic with an effective moment per formula unit of 0.4 μ_B at 4.5 K, rising to 1.4 μ_B at 300 K. A Curie−Weiss law did not fit the data across the whole temperature range (Figure 8a). However, over the range 15−200 K, a power law dependence of the form $\chi = mT^{-\alpha}$, where $\alpha = 0.34 \pm 0.01$, was observed (Figure 8b). This behavior has been reported before in highly conducting organic materials.[20] It is attributed to the effects of defects in linear chain structures, and it is likely that we have a segregated stacking in the present material, giving rise to a disordered linear chain structure.

A weak paramagnetic moment was also measured for the complex **8**−TCNQ. This did not show Curie−Weiss behavior except in the very low temperature region but, at least qualitatively, exhibited the temperature variation predicted by the Bonner−Fisher model for an $S = {}^1/_2$ linear chain antiferromagnet with J between 70 and

(20) (a) Bulaevski, L. N.; Zyarykina, A. V.; Karimov, Yu.S.; Lyubovski R. B.; Shchegolev, I. F. *Sov. Phys. JETP* **1972**, *62*, 725. (b) Torrance, J. B. In *Low Dimensional Conductors and Superconductors*; Jérome, D., Caron, L. G., Eds.; Plenum: New York, 1987.

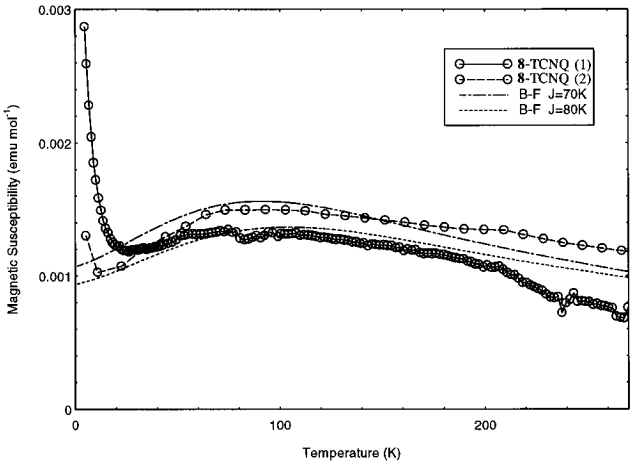

Figure 9. Static susceptibility of **8**−TCNQ as a function of temperature together with the predictions of the Bonner−Fisher model for various J values. The two independent sets of data are labeled **8**−TCNQ (1) and **8**−TCNQ (2).

80 K (Figure 9). Although a detailed fit over the whole temperature range could not be achieved, the discrepancy is of the same magnitude as the systematic differences between independent measurements [e.g., **8**−TCNQ (1) and **8**−TCNQ (2) shown in Figure 9]. In the case of such a very weak paramagnet, the corrections to the data for the diamagnetic contribution of the balance bucket are extremely large. A small amount of impurity entering the system or slight errors in alignment of the bucket in the field between sample and baseline runs could account for these differences. However, the overall broad maximum is always reproduced. The Curie tail probably arises from unpaired spins at defects at the end of the chain lengths.

Conclusions

A series of extensively conjugated TTF analogues containing a central 2,2′-ethanediylidene group have been studied. The compounds are excellent π-electron donors yielding cation radicals and dications at low oxidation potentials, in agreement with previous studies on TTF vinylogues. ESR and proton ENDOR spectra demonstrate that the bulk of the spin population resides in the central $S_2C{=}C{-}C{=}CS_2$ part of the π-system. The first X-ray crystal structure of a charge-transfer complex of a TTF vinylogue with TCNQ has been obtained, which reveals a mixed-stack structure. Attempts to electrocrystallize cation radical salts of donors **5**, **6**, and **8**−**11** with inorganic anions has so far failed to provide single crystals. It is possible that the donors undergo some decomposition under the conditions and the time scale (>1 week) required for the electrocrystallization process.

Acknowledgment. The work in the UK was funded by EPSRC; the work in Basel was supported by the Swiss National Science Foundation.

CM940376+